Articles

Processing Effects on the Compositional Depth Profile of Ferroelectric Sol−Gel Ca−$PbTiO_3$ Thin Films

R. Sirera,[†] D. Leinen,[‡] E. Rodríguez-Castellón,[§] and M. L. Calzada*,[||]

Dpt. Química y Edafología, Univ. de Navarra, 31080 Pamplona, Spain; Dpt. de Física Aplicada, Univ. de Málaga, 29071 Málaga, Spain; Dpt. de Química Inorgánica, Univ. de Málaga, 29071 Málaga, Spain; and Inst. Ciencia de Materiales de Madrid, ICMM−CSIC, Cantoblanco, 28049 Madrid, Spain.

Received November 23, 1998. Revised Manuscript Received August 31, 1999

$Pb_{0.76}Ca_{0.24}TiO_3$ thin films have been prepared by sol−gel on Pt/TiO_2/(100)Si substrates. Films deposited from a stoichiometric solution and a solution with a 10 mol % excess of Pb were subjected to a thermal treatment at 650 °C for 720 s with a heating rate of 8 °C/s and to a rapid thermal treatment (RTP) at 650 °C for 50 s with a rate of 30 °C/s, respectively. Chemical composition in surface, in depth, and at the bottom interface with the substrate of the films were studied by X-ray photoelectron spectroscopy (XPS) combined with Ar^+ depth profiling. XPS results were compared with those obtained by Rutherford backscattering spectroscopy (RBS). To make the interpretation of the XPS data easier and to complete them, the structure and microstructure of the films were monitored by grazing incidence X-ray diffraction analysis (GIXRD) and scanning electron microscopy (SEM). The RTP film prepared with a Pb excess developed a single perovskite phase with preferred orientation and a uniform depth profile in composition. The other film also has a single perovskite phase, but with a random orientation, and presents a nonuniform distribution of Pb across the film thickness. Whereas the latter film does not have a good ferroelectric response, the former does. After poling it, values of remanent polarization of $P_r \sim 25\ \mu C/cm^2$, coercive field of $E_c \sim 75$ kV/cm, and pyroelectric coefficients of $\gamma \sim 2.5 \times 10^{-8}$ were obtained.

Introduction

Ferroelectric thin films have attracted much attention during the last years, owing to their possible integration into multifunctional microelectronic devices.[1] The aim of using these materials in the microelectronic technology is to exploit some of their properties such as spontaneous polarization when they are integrated into nonvolatile ferroelectric random-access memories (NVFRAMs), pyroelectricity for infrared sensors, or piezoelectricity in microelectromechanical systems (MEMS). For bulk materials, their electrical response is closely linked to composition, structure, and microstructure. However, when the ferroelectric material is deposited as a thin layer, the number of factors affecting its performance substantially increases. In this case, heterostructure is an additional factor that plays an important role in film devices. The term heterostructure includes substrate, buffer layer, electrode, active (ferroelectric) layer, and interface.

Composition, structure, microstructure, and heterostructure of a thin-film-based device are conditioned by the underlaying substrate and the deposition method.[2,3] Available substrates on which the ferroelectric layer is deposited are those used in the microelectronic industry. So, the majority of the research work on ferroelectric thin films is focused on their applications when they are integrated into silicon. Some reports have considered other substrates, particularly when a preferred orientation of the active layer is desired.[4,5] However, from the point of view of applications, authors observe that substrates different from silicon are hardly technologically interesting.[6] Therefore, it seems more appropriate to regulate parameters of deposition methods to control characteristics and properties of thin films. Among the different deposition techniques, sol−gel is a method that offers significant advantages over others, such as stoichiometric control of complex oxides and uniform incorporation of dopants. Moreover, it is relatively rapid,

* To whom correspondence should be addressed. Telephone: 34 91 334 90 62. Fax: 34 91 372 06 23. E-mail: lcalzada@icmm.csic.es.
[†] Univ. de Navarra.
[‡] Dpt. de Física Aplicada, Univ. de Málaga.
[§] Dpt. de Química Inorgánica, Univ. de Málaga.
[||] ICMM−CSIC.

(1) Auciello, O.; Ramesh, R. *MRS Bull.* **1996**, *21* (7), 29.
(2) Kushida, K.; Udayakumar, K. R.; Krupanidhi, S. B.; Cross, L. E. *J. Am. Ceram. Soc.* **1993**, *76* (5), 1345.
(3) Auciello, O.; Ramamurthy, R. *MRS Bull.* **1996**, *21* (6), 21.
(4) Kim, S.; Baik, S. *Thin Solid Films* **1995**, *266*, 205.
(5) Seifert, A.; Lange, F. F.; Speck, J. S. *J. Mater. Res.* **1995**, *10* (3), 680.
(6) Dat, R.; Lichtenwalner, J.; Auciello, O.; Kingon, A. I. *Appl. Phys. Lett.* **1994**, *64* (20), 2673.

10.1021/cm980770y CCC: $18.00
Published on Web 11/04/1999

inexpensive, and compatible with semiconductor technologies.[7,8] The main disadvantage of this technique is the difficulty in obtaining conformational and thick deposits.

Lead titanate zirconate, $Pb(Zr,Ti)O_3$ (PZT), has been the ferroelectric composition most widely studied as thin films. However, pure lead titanate ($PbTiO_3$) also seems to be a promising ferroelectric, pyroelectric, and piezoelectric material, because it has a large spontaneous polarization (P_s), a relatively low dielectric constant, ϵ, and a large electromechanical anisotropy. However, its coercive field, E_c, is so large that it requires high electric fields for poling, much higher than those used in microelectronic devices (≤3 V). Partial substitution of Pb by appropriate amounts of Ca produces a considerable decrease of E_c, while keeping or increasing the piezoelectric anisotropy and maintaining large values of spontaneous polarization, P_s.[9−11]

In this paper, we use an aquo-diol based sol−gel process, previously reported by the authors for the preparation of $Pb_{0.76}Ca_{0.24}TiO_3$ (PCT) thin films.[12,13] The films deposited from sol−gel solutions are amorphous and require a thermal treatment for their crystallization into the desired phase. In the case of lead−perovskite thin films, volatilization of lead during annealing occurs, which could produce an unbalance in the final composition or the formation of lead-deficient phases. Besides, during annealing, an interdiffusion process may occur among the different layers forming the film heterostructure. This phenomenon damages the material and its electric response. To reduce these drawbacks, lead excess is added to the solutions and rapid thermal processings (RTP) are applied.[14] However, elimination of the knotty points that appear during preparation of thin films requires a good knowledge of their characteristics. Traditional analytical techniques used for the study of materials [X-ray diffraction (XRD), scanning electron microscopy (SEM), transmission electron microscopy (TEM), etc.] are used for the study of films. Nevertheless, other techniques, mainly spectroscopic techniques used to study surfaces, are quickly increasing their role in the study of thin films. Techniques such as X-ray spectroscopies [X-ray fluorescence (XRF), X-ray absorption spectroscopy (XAS), etc.], electron and ion spectroscopies [X-ray photoelectron spectroscopy (XPS), atomic emission spectroscopy (AES), secondary-ion mass spectroscopy (SIMS), etc.], and Mössbauer spectroscopy or Rutherford backscattering spectroscopy (RBS) have successfully been applied to the analysis of thin films[15,16] in recent years.

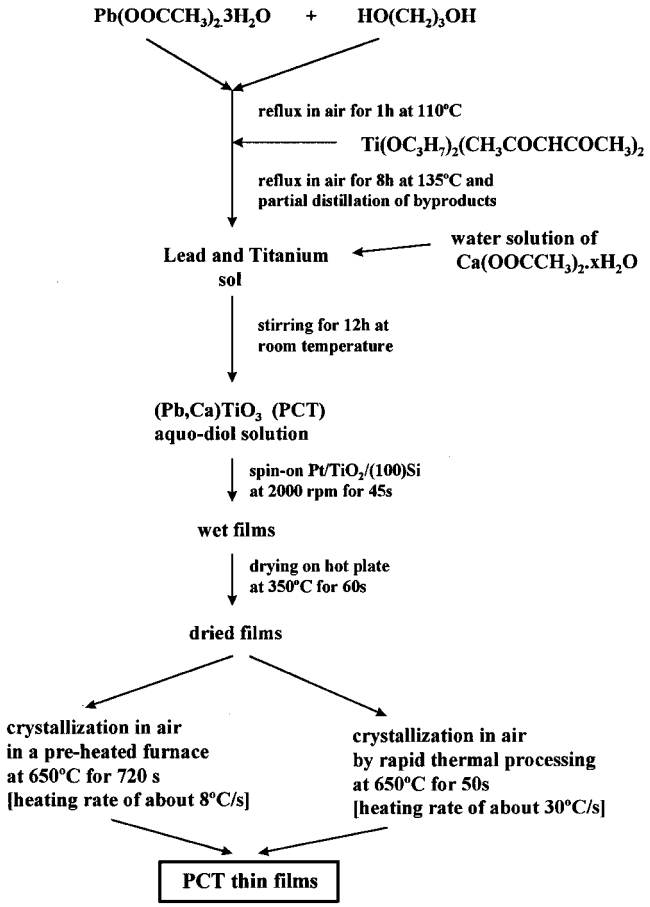

Figure 1. Preparation scheme of the $(Pb,Ca)TiO_3$ thin films.

In this context, XPS combined with inert ion depth profiling can give valuable information, with high depth resolution, about compositional and chemical changes. XPS can be used as a tool for the control of stoichiometry and compositional homogeneity of the material, and it is of special interest in the interface regions between the different layers integrating the heterostructure of ferroelectric thin film devices.

We report about the compositional, structural, microstructural, and heterostructural characteristics of sol−gel PCT thin films on $Pt/TiO_2/(100)Si$ substrates. Different processing conditions were used for preparing these films. The effect of these conditions on the final characteristics of the films is studied by means of XPS combined with inert ions depth profiling. The results obtained with this technique together with those resulting from other characterization techniques (XRD, SEM, and RBS) allowed us to select the optimum conditions for the preparation of these ferroelectric thin films.

Experimental Section

The scheme of the chemical processing for the preparation of calcium-modified lead titanate thin films, with nominal composition of $Pb_{0.76}Ca_{0.24}TiO_3$, is presented in Figure 1. A reaction method of two steps was followed to synthesize the PCT solution.[12] First, lead acetate trihydrate, $Pb(OOCCH_3)_2 \cdot 3H_2O$, was dissolved in 1,3-propanediol, $HO(CH_2)_3OH$, in a 1:5 molar ratio of lead to diol and refluxed at 110 °C in air for 1 h. After a slight cooling, titanium isopropoxide bisacetylacetonate, $Ti(OC_3H_7)_2(CH_3COCHCOCH_3)_2$, was added in a 0.76:1 molar ratio of lead to titanium. This solution was refluxed in air at 135 °C for 8 h, and a partial distillation of

(7) Tuttle, B. A.; Schwartz, R. W. *MRS Bull.* **1996**, *21* (6), 49.
(8) Schwartz, R. W. *Chem. Mater.* **1997**, *9*, 2325.
(9) Calzada, M. L.; Mendiola, J.; Carmona, F.; Ramos, P.; Sirera, R. *Mater. Res. Bull.* **1996**, *31* (4), 413.
(10) Calzada, M. L.; Sirera, R.; Ricote, J.; Pardo, L. *J. Mater. Chem.* **1998**, *8* (1), 111.
(11) Kholkin, A. L.; Calzada, M. L.; Ramos, P.; Mendiola, J.; Setter, N. *Appl. Phys. Lett.* **1996**, *69* (23), 3602.
(12) Sirera, R.; Calzada, M. L. *Mater. Res. Bull.* **1995**, *30* (1), 11.
(13) Calzada, M. L.; Sirera, R. *J. Mater. Sci.-Mater. Elect.* **1996**, *7*, 39.
(14) Sirera, R.; Martín, M. J.; Calzada, M. L. *Bol. Soc. Esp. Cerám. Vidrio* **1998**, *37* (2−3), 109.
(15) Bruynseraede, Y.; Schuller, I. K. *MRS Bull.* **1992**, *17* (12), 20
(16) Leinen, D.; Caballero, A.; Fernández, A.; Espinós, J. P.; Justo, A.; González-Elipe, A. R.; Martin, J. M.; Maurin-Perrier, B. *Thin Solid Films* **1996**, *272*, 99.

byproducts was carried out. Thus, a first lead and titanium sol was obtained with a concentration, density, and pH of ∼1.3−1.5 M, ∼1.3−1.5 g/cm^3, and ∼6.0, respectively. In the second step, the incorporation of calcium into this system was carried out through an aqueous solution of calcium acetate $Ca(OOCCH_3)_2{\cdot}xH_2O$, in a 0.24:1 molar ratio of calcium to titanium and a 5:1 molar ratio of water to diol. After being vigorously stirred for 12 h at room temperature, stable aquo-diol solutions were obtained with concentrations of ∼0.9 M. By use of these experimental conditions, a stoichiometric solution with the nominal composition of $Pb_{0.76}Ca_{0.24}TiO_3$ and another containing a 10 mol % excess of lead were synthesized.

A single coating of these solutions was deposited by spin-on at 2000 rpm for 45 s onto Pt/TiO_2/(100)Si substrates. Surface roughness of these substrates was previously measured by profilemetry. The coated wet layers were dried on a hot plate at 350 °C for 60 s, to remove residual solvent and to promote partial pyrolysis of the organic components. Two types of thermal treatment were applied to the films in order to enhance the crystallization of the (Pb,Ca)TiO_3 perovskite phase. The first treatment consisted in inserting the dried film in a preheated conventional furnace at 650 °C for 720 s, in air. The average heating rate of this treatment was about 8 °C/s. The other thermal treatment was a rapid thermal processing (RTP) in air at 650 °C for 50 s, with a heating rate of about 30 °C/s. This treatment was carried out using infrared heat lamps in a commercial RTP system, model JETSTAR 100T, manufactured by J. I. P. E. L. E. C.

The nomenclature used for the films analyzed in this work will be, hereinafter, as follows:

Film A. Deposited from the stoichiometric solution and crystallized in a preheated furnace at 650 °C for 720 s, with a heating rate of ∼8 °C/s.

Film B. Deposited from a solution with a 10 mol % excess of lead and crystallized by RTP, with a heating rate of ∼30 °C/s.

Grazing incidence X-ray diffraction (GIXRD) was used to study the crystalline phases developed in these films.[17] A Siemens D500 powder diffractometer with a flat LiF monochromator in the diffracted beam was used. A Cu anode, operating at 40kV and 25 mA and a scanning speed of 0.15 °C min^{-1}, was used. Diffraction patterns were recorded between 20 and 50 °C, using an incidence angle of 2° to avoid signal from the underlaying substrate. Scanning electron microscopy (SEM) images were taken from random regions of the film surfaces in order to view the film microstructures. Cross-sectional images were also obtained to distinguish the different layers forming the heterostructure of the material. A Hitachi S-800 microscope was used for such observations. RBS data here presented were collected following the experimental procedure previously reported by Martin et al.[18] These results were compared with those obtained by XPS.

XPS measurements were carried out with a PHI 5700 equipment. Survey and multiregion spectra were recorded of Pb 4f, Ca 2p, Ti 2p, O 1s, Pt 4f, Si 2p, and C 1s photoelectron peaks and Pb MNN, Ti LMV, and O KVV Auger peaks. The atomic concentrations were calculated from the photoelectron peak areas, using Shirley[19] background subtraction and sensitivity factors provided by the spectrometer manufacturer PHI.[20] All binding energies refer to Ca2$p_{3/2}$ at 347.0 eV. Depth profiling was carried out by 4 keV Ar^+ bombardment and a current density of ∼3 μA cm^{-2}. Data were recorded after 1 min of 4 keV Ar^+ sputter cleaning of the film surface, to eliminate adsorbed carbon and other species. After the surface was cleaned, depth profiles of the samples were obtained up to the undermost Si substrate, taking data after each 2 or 5 min of 4 keV Ar^+ sputtering. The in-depth scale of 0.5 nm/min was assumed to be equivalent to the sputter rate of Ta_2O_5 under the same sputter conditions. Severe changes in sputtering yield between the sample under study and Ta_2O_5 are taken into account in the discussion.

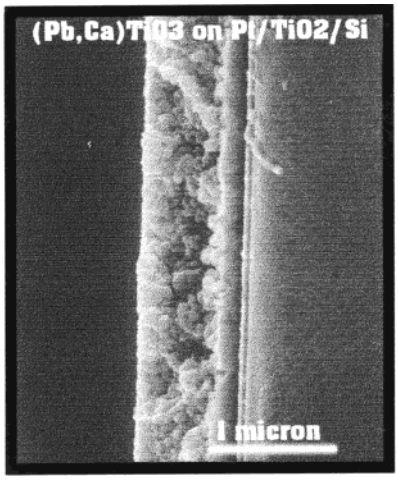

Figure 2. SEM image of the cross section of a (Pb,Ca)TiO_3 thin film onto Pt/TiO_2/(100)Si substrate.

Top platinum electrodes of about 500 μm in diameter were deposited onto the top surfaces of the crystalline PCT films, to carry out electrical characterization. Hysteresis loops were traced using a modified Sawyer−Tower circuit and an oscilloscope. A sinusoidal signal with an amplitude of 320 kV/cm and a frequency of 1 Hz was used for these measurements. Coercive fields, E_c, and remanent polarizations, P_r, were obtained from the measurement of switching curves, using the method of pulses described by Ramos et al.[21] This procedure consisted of applying to the films 10^4 square pulses of ∼320 kV cm^{-1} in amplitude and 200 μs in width, with an interval of 20 μs. Subsequently, two equal reading pulses of opposite sign were used to measure the switching current. In this way, the contribution of possible nonferroelectric charges, which would be included in the hysteresis loops, is eliminated. Pyroelectric coefficients were calculated from pyroelectric currents after a triangular thermal wave of ±1.5 °C and 7 × 10^{-3} Hz with an effective gradient of 2.6 °C/min[22] was applied to the films.

Results

Figure 2 shows, as an example, a cross-sectional image obtained by scanning electron microscopy of film B. As it can be seen, the average thickness of the PCT film, free of defects and prepared after a single deposition and thermal treatment, is about 0.5 μm. The heterostructure consists, from top to bottom, of the PCT film, a Pt-sputtered bottom electrode about 1500 Å thick, a TiO_2-sputtered buffer layer about 500 Å thick, and the (100)Si substrate. Roughness, measured by profilemetry, of the Pt bottom electrodes used for the preparation of films A and B, was very similar for both cases, ∼0.025 ± 0.003 μm. The scanning electron images shown in Figure 3a,b correspond to the microstructures of films A and B, respectively. Both microstructures are constituted by clusters (association of grains) with inter- and intracluster porosity. The highest degree of porosity is observed in the microstructure of film A. The clusters of this film are smaller than those in film B. XRD

(17) Mendiola, J.; Calzada, M. L.; Sirera, R.; Ramos, P. *Proceedings of the 4th International Conference on Electroceramics & Application*; Waser, R, Hoffman, S., Bonnenberg, D., Hoffman, Ch., Eds.; Aachen, Germany, 1994; Vol. 1, p 327.

(18) Martin, M. J.; Calzada, M. L.; Mendiola, J.; Da Silva, M. F.; Soares, J. C. *J. Sol−Gel Sci. Technol.* **1998**, *13*, 843.

(19) Shirley, D. A. *Phys. Rev.* **1972**, *B5*, 4709.

(20) Physical Electronics, 6509 Flying Cloud Drive, Eden Prairie, MN 55344.

(21) Ramos, P.; Mendiola, J.; Carmona, F.; Calzada, M. L.; Alemany, C. *Phys. Status Solidi A* **1996**, *156*, 119.

(22) Jimenez, R.; Calzada, M. L.; Mendiola, J. *Thin Solid Films*, in press.

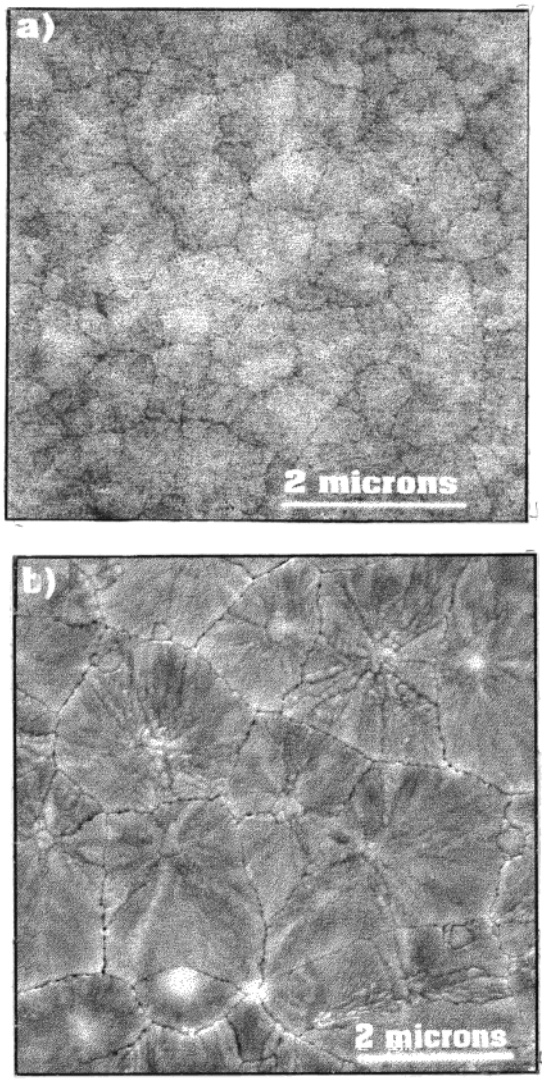

Figure 3. SEM images of the top surfaces of films (a) A and (b) B.

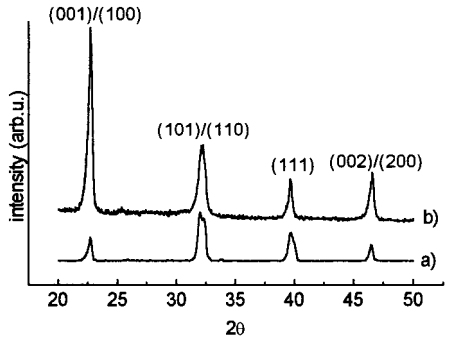

Figure 4. GIXRD patterns of crystalline films (a) A and (b) B.

patterns of films A and B are depicted in parts a and b of Figure 4, respectively. It is shown the development in both films of a crystalline calcium-modified lead titanate phase with a perovskite structure. This perovskite has a random orientation for film A, whereas the perovskite formed in film B has a preferred {001}/{100} orientation. Only one crystalline phase was observed in the films.

For the study of the heterostructure of the films, both the thickness of the Pt electrode−ferroelectric film interface and the thickness and composition of the ferroelectric layer have been determined. These are the parameters that affect more the ferroelectric response of these materials. They have been calculated from XPS data and compared with those obtained by RBS.

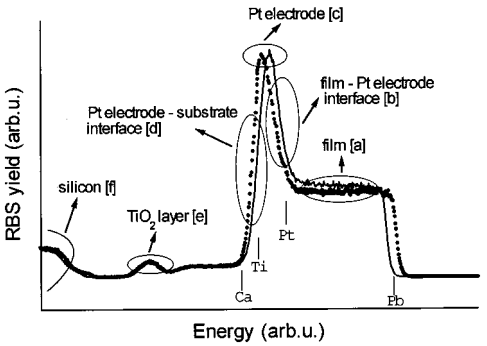

Figure 5. RBS spectra of films A (—) and B (••••). The approximate energies of the backscattered He^+ by Ca, Ti, Pt, and Pb are indicated in the figure (these change slightly for each film). The zones of the spectra from which information on the layered heterostructure can be obtained are also marked.

Table 1. Pb/Ca Ratios and Thicknesses of the Perovskite Layer and Bottom Interface of Films A and B Obtained from the RBS Spectra in Figure 5

film[a]	Pb/Ca[b]	film thickness [a] (Å)	film−Pt electrode interface thickness [b] (Å)
A	~0.66/0.24	~4400	~700
B	~0.77/0.24	~4000	~600

[a] Partially reported by Martin et al.[18] [b] [Pb]/[Ca] = average atomic ratio measured in the bulk ferroelectric film

RBS spectra were simulated from the data recorded by RBS technique[18] and using the RUMP software.[23] Some assumptions have to be taken into account for the analysis of these data. First, it has been assumed that the presence in the samples of different layers with variable composition, as well as the simulations, was performed with layer thickness in atoms per square centimeter. These units have been converted to nanometers by considering a bulk density of the films equal to that calculated from the atomic densities of each element of the $Pb_{0.76}Ca_{0.24}TiO_3$ perovskite. Therefore, factors such as formation of perovskite defects, porosity, or second phases have not been considered. Second, the Pt signal overlaps the signals of Ca and Ti. So, calcium and titanium concentrations cannot be estimated and have been considered unchanging and equal to those of the nominal perovskite ($Pb_{0.76}Ca_{0.24}TiO_3$). With these assumptions, a semiquantitative calculation of the Pb concentration of the films can be made. Figure 5 shows the spectra corresponding to films A and B. Regions of the spectra from which the main information can be inferred are marked in the figure. The thickness [b] can be estimated from the slope of the straight line formed by the experimental data of the zone. A higher slope indicates a thinner interface and a lower slope indicates a thicker interface. The Pb concentration is calculated from the height of the Pb signal, [a]. Table 1 shows these results for films A and B. Note that film A has a larger thickness of the ferroelectric layer and of the interface

(23) Doolittle, L. R. *Nucl. Inst. Methods* **1984**, *B9*, 334.

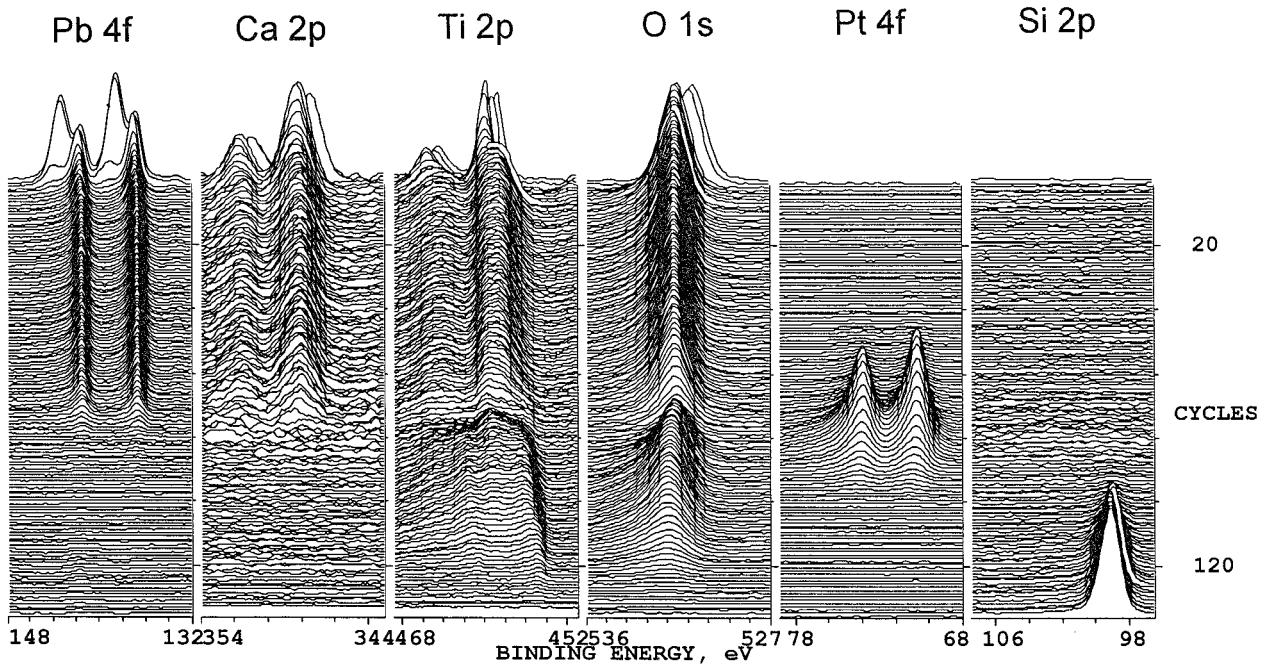

Figure 6. XPS spectra recorded during Ar^+ depth profiling of a (Pb,Ca)TiO_3 thin film deposited onto Pt/TiO_2/(100)Si. For explanation, see text.

than film B. Also, the Pb/Ca ratio calculated from the RBS spectrum of film A indicates that Pb has been lost during its thermal treatment. Pb loss is also detected in film B, because this film was deposited from a solution with a 10 mol % excess of Pb (see Table 1).

Figure 6 shows, as an example, all of the XPS spectra recorded for film B during the depth profile from top to bottom, with increasing sputter time in sequences of 5 min. From these spectra and those measured for film A, the atomic ratios have been calculated and plotted-versus Ar^+ sputter time in Figure 7. Ratios of Pb to Ca or Ti are given in Table 2.

The XPS analysis indicates that both films have a large contamination at their surfaces, about 30% of carbon in atomic concentration, which drops after 1 min of Ar^+ sputter cleaning to about 3%. Just after the elimination of this contaminated layer, the surface of film B shows a Pb/Ca ratio equal to the nominal one, whereas the surface of film A is slightly deficient in Pb (see Table 2). The chemical formula determined from the XPS atomic concentrations at 1 min of 4 keV Ar^+ sputter cleaning for films A and B are $Pb_{0.68}Ca_{0.32}Ti_{0.94}O_{2.72}$ and $Pb_{0.76}Ca_{0.24}Ti_{0.82}O_{2.52}$, respectively. In addition, binding energies of Pb $4f_{7/2}$, Ca $2p_{3/2}$, Ti $2p_{3/2}$ and O 1s at 138.7, 347.0, 458.6, and 530.1 eV, and modified Auger parameters of Pb, Ti, and O at 227.3, 872.2, and 1042.2 eV, respectively, were determined by XPS for the film surfaces. These values are in good agreement with values given in the literature[24,25] for nonmodified lead titanate, $PbTiO_3$. Afterward, depth profiling was carried out by 4 keV Ar^+ etching. Prolonged Ar^+ bombardment leads to severe changes in the film surface analyzed by XPS. Ar^+ bombardment causes a preferential loss of O and Pb in the sample surface, i.e., a reduction of Pb to the metallic state and thereafter of Ti to lower oxidation states. A lower energy (<4 keV) Ar^+ bombardment could be used for decreasing preferential sputtering. However, lower energies lead to low sputtering rates without a considerable reduction of the lead removal. This effect is well-known for different titanates subjected to ion bombardment.[26] In the case of $PbTiO_3$, the preferential

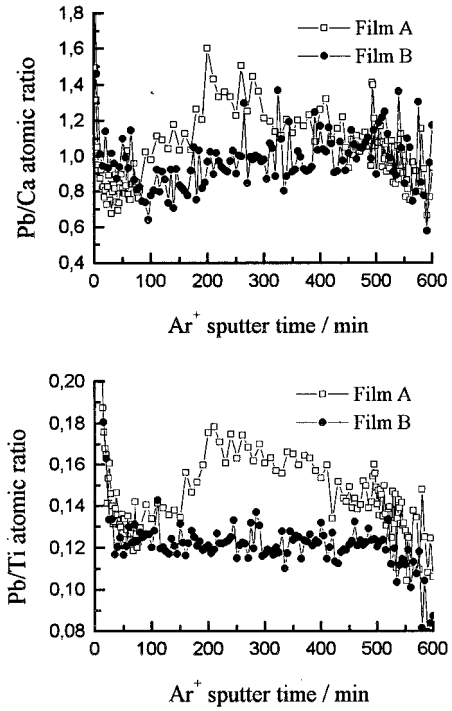

Figure 7. Pb/Ca (top) and Pb/Ti (bottom) atomic ratios calculated from XPS data for the different exposed surfaces due to 4 keV Ar^+ depth profiling of films A and B. Lines between data points are drawn to guide the eye. The relative errors of data points are about 20% for the Pb/Ca ratio and 5% for the Pb/Ti ratio.

(24) Murata, M.; Wakino, K; Ikeda, S. *J. Electron. Spectrosc.* **1975**, *6*, 459.

(25) Leinen, D.; Fernández, A.; Espinós, J. P.; González-Elipe, A. R. *Surf. Interface Anal.* **1993**, *20*, 941.

(26) Leinen, D.; Fernández, A.; Espinós, J. P.; González-Elipe, A. R. *Appl. Phys.* **1996**, *A63*, 237.

Table 2. Atomic Ratios from the Different Exposed Surfaces Due to 4 KeV Ar^+ Depth Profiling of Films A and B

region:time at 4 keV Ar^+(min)[a]	film A		film B	
	Pb/Ca	Pb/Ti	Pb/Ca	Pb/Ti
atm. ambient contam. surf. (~30% carbon): 0	0.74/0.26	0.49/0.51	0.83/0.17	0.58/0.42
sputter-cleaned surf. (remain. ~1% carbon): 1	0.68/0.32	0.42/0.58	0.76/0.24	0.48/0.52
steady-state concn of ion bombard. depth profil.: 100	0.50/0.50	0.12/0.88	0.45/0.55	0.12/0.88
middle of ferroelectric layer: 250/250[b]	0.58/0.42	0.15/0.85	0.48/0.52	0.11/0.89
preinterf. reg. (at 16% of total Pt intens.): 532/550[b]	0.49/0.51	0.14/0.86	0.47/0.53	0.10/0.90
interface region (at 50% of total Pt intens.): 575/585[b]	0.50/0.50	0.12/0.88	0.42/0.58	0.10/0.90

[a] Uncertainty in the measurements is about 5% for lead and titanium concentrations and about 18% for calcium concentration. [b] For films A and B, respectively.

loss of lead is ascribed to the high volatility of this element on the sample surface owing to the thermal spike caused by the impinging ions.[25,27] The first two spectra of Figure 6 (top of the figure) correspond to the situation before depth profiling, i.e., after 1 min of Ar^+ sputter cleaning. A reduction of around 30% of Pb to the metallic state can be observed. After about 50 to 100 min of Ar^+ bombardment, a steady-state situation is reached. Pb is in metallic state and Ti is reduced to lower oxidation states, whereas the oxidation state of Ca is not affected by Ar^+ bombardment, as can be seen in Figure 6 from the Ca 2p peak. The initial change in binding energy of all peaks, i.e., between second and third spectra (at the top of Figure 6), is due to a charge effect as a consequence of Ar^+ bombardment. It has to be taken into account that in the steady-state situation of Ar^+ bombardment the composition of the sample surface has been completely changed, as a result of the preferential loss of lead and oxygen during the sputtering. At this point, this surface consists mainly of a reduced phase of titanium oxide. Metallic Pb is found in a very low concentration, similar to that found for Ca (see Figure 7 and Table 2). Further depth profiling shows, below the ferroelectric film, the Pt electrode, the TiO_2 buffer layer, and the Si substrate, but no SiO_2 layer is observed between the TiO_2 and the Si. This is inferred from the absence of a peak at about 10^3 eV corresponding to silicon oxide in the Si 2p region (Figure 6).

As already pointed out, a consequence of Ar^+ bombardment is not only the chemical reduction of Pb and Ti but also a preferential loss of Pb. Figure 8 shows the evolution of the peak areas versus sputter time, i.e., relative depth, of the two films. In this plot can clearly be seen how Pb is lost preferentially and, to a lesser extent, Ca during the first 100 min of Ar^+ sputtering. Thereafter, a steady state situation is reached, which is similar for both films; only a slightly higher Ca concentration is obtained for film B (see Table 2). After about 200 min of depth profiling, an increase of Pb intensity can be observed for film A, whereas no significant changes of the XPS intensities are remarked for film B. This is clearly distinguishable in Figure 7 from the differences in the Pb/Ti ratios between films A and B. A higher amount of Pb is also detected in the interface with the Pt electrode of film A, when compared with film B (see also Table 2). Atomic ratios in this interface region (Pt electrode−ferroelectric layer) have been calculated for both films, at 16% and 50% of the total Pt intensity. These values are included in Table 2. They show, in comparison with the values obtained for the ferroelectric layer, that the Pb/Ti ratio of film A drops progressively more and more from a thickness of about 100 nm to the interface region, whereas it remains constant for film B (Figure 7). Nevertheless, film A still has a concentration of Pb in the interface region higher than that of film B. In fact, comparing the depth profiles of Figure 8 obtained for both films, one can clearly observe that the latter film is more homogeneous than the former one.

Figure 9 shows the ferroelectric hysteresis loops corresponding to films A and B. The loop of film B is better defined than that of film A. Remanent polarizations, P_r, and coercive fields, E_c, were not obtained from these curves, because the loop of film A has a large contribution of leakage currents. The latter also shows a considerable bias field. To avoid contribution of these nonferroelectric charges, P_r and E_c have been obtained from the switching curves as was already explained in the former section. P_r, E_c, and pyroelectric coefficients measured for these films are summarized in Table 3.

Discussion

The two types of films studied here, A and B, have different depth profiles (see Figure 8) that produce different ferroelectric responses, as shown in the hysteresis loops of Figure 9. Three main areas of interest can be identified in the loop of film A, if compared with the loop of film B: first, the shift of the hysteresis curve; second, the large contribution of leakage currents (observed by the roundness of the loop); and third, the lower remanent polarization, better observed when it is calculated from switching measurements (see Table 3). The XPS data analyzed in this work explain these results and relate them to the processing parameters.

After removal of the carbon-contaminated top surface layer, XPS depth profiling shows differences in composition between films A and B. Whereas film B, at its cleaned surface, has a Pb/Ca ratio equal to that of the nominal composition, film A has a lead deficiency (Table 2). This defect of Pb is due to its volatility at the annealing temperatures used for the crystallization of film A. The incorporation of a lead excess into the precursor solution of film B compensates this lead loss, obtaining a film with a composition close to that of the stoichiometric perovskite ($Pb_{0.76}Ca_{0.24}TiO_3$). This film is also homogeneous in depth due to the rapid heating rate used for its crystallization. On the contrary, the long duration thermal treatment used for film A provides enough time for diffusion or volatilization of some

(27) Mukhopadhyay, S. M.; Chen, T. C. S. *J. Phys. D: Appl. Phys.* **1995**, *28*, 2170.

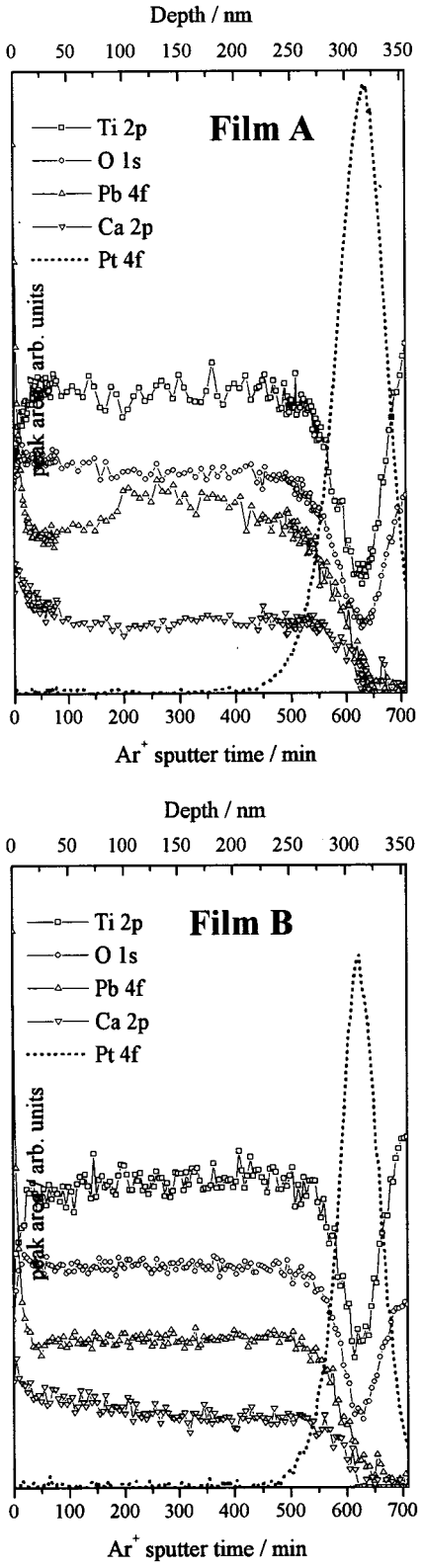

Figure 8. Photoelectron peak intensities during depth profiling with 4 keV Ar^+ of the (Pb,Ca)TiO_3 thin films A and B deposited on Pt/TiO_2/(100)Si.

elements of the material.[28] So, film A has a lead excess close to the interface region with the Pt electrode. At this interface, a higher reaction degree is observed between the ferroelectric layer and the electrode for film A than that for film B (Figure 5). Then, the heating rate used here for the crystallization of film A (8 °C/s) is rapid enough for not developing in it appreciable quantities of nonferroelectric pyrochlore or fluorite phases,[29,30] but not for avoiding Pb volatilization and Pb diffusion. The loss and migration of Pb produce charge defects (lead and oxygen vacancies and holes)[31] that justify the shift of the hysteresis loop and the lower values of remanent polarization and higher values of coercive fields of film A than those of film B.[32,33] The expected composition and depth profile homogeneity of film B contribute to its well-defined hysteresis loop (Figure 9).

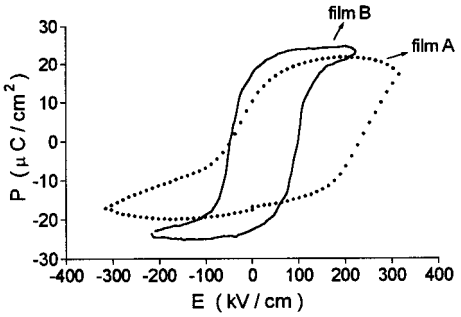

Figure 9. Hysteresis loops of films A and B, measured at 1 Hz.

Table 3. Dielectric, Ferroelectric and Pyroelectric Parameters Obtained for Films A and B

film	ϵ_r	P_r (μC/cm^2)[a]	E_c (kV/cm)	γ (C/cm °C) without poling	γ (C/cm °C) after poling
A	∼160	∼13	∼125		$\sim 0.8 \times 10^{-8}$
B	∼600	∼25	−75	$\sim 2.8 \times 10^{-9}$	$\sim 2.5 \times 10^{-8}$

[a] Values of P_r obtained from switching current measurements (see Ramos et al.[21]). P_r values directly obtained from the hysteresis loops of Figure 8 are not real, especially for the film A, because of the contribution of leakages (∼20 and ∼25 μC/cm^2 for the A and B films, respectively).

The thickness trend obtained by XPS is in accordance with that of RBS results, but the values calculated from both techniques are different (Table 1 and Figure 8). In the case of the XPS analysis, differences are due to the preferential sputtering effect of lead during depth profiling. Pb and PbO are lost preferentially and with ease from the film surface, leaving an altered layer consisting mainly of a reduced titanium oxide phase. This means that the ferroelectric layer under the scale of Figure 8 appears thinner than it really is. A correction factor for this difference with respect to depth profiling of Ta_2O_5 may be on the order of nearly 2, but it cannot be given with any accuracy. Neither are the thicknesses deduced from the RBS data precise, because it is not easy to know the bulk density of the ferroelectric layer, which is necessary for the simulation of the RBS spectra.

The thickness of the Pt electrode was determined by XPS for each film by the measurement of the fwhm of the Pt intensity versus sputter time (Figure 8) and by

(28) Hoffman, M.; Goral, J. P.; Al-jassim, M. M.; Echer, C. *J. Vac. Sci. Technol. A* **1992**, *10* (4), 1584.
(29) Calzada, M. L.; Jiménez, R.; Ramos, P.; Martín, M. J.; Mendiola, J. *J. Phys. IV (France)* **1998**, *8*, 53.
(30) Hu, H.; Shi, L.; Kumar, V.; Krupanidhi, S. B. *Ceram. Trans.* **1992**, *25*, 113.
(31) Jaffe, B.; Cook, W.R; Jaffe, H. *Piezoelectric Ceramics*; R. A. N. Publishers: Marietta, OH, 1971.
(32) Waser, R. *NATO ASI Series E: Appl. Sci.* **1995**, *284*, 223.
(33) Robels, U.; Calderwood, J. H; Arlt, G. *J. Appl. Phys.* **1995**, *77* (8), 4002.

taking into account the relative sputter rate for Pt (factor 2.2)[34] with respect to Ta_2O_5 at 4 keV Ar^+. The thicknesses of the Pt electrodes are 207 and 162 nm for films A and B, respectively. Integration of the Pt intensity with depth shows that in film A the total amount of Pt is a factor of ~1.2 higher than that in film B. This indicates slightly different conditions during the sputter deposition of Pt on TiO_2/(100)Si in both films.

Finally, it should be mentioned that one has to be careful with the interpretation of depth profiles carried out with 4 keV Ar^+ sputtering of materials where strong preferential sputter effects are involved, as in our case for Pb. First, preferential sputtering of Pb in combination with the overall reduction of the mixed oxides, i.e., preferential loss of oxygen atoms, can lead to an unexpected depth profile of constant oxygen concentration.[27] Thus, the preferential loss of O during 4 keV Ar^+ profiling is not evident from a concentration depth profile. In that case, preferential sputtering of Pb leads to a higher relative Ti concentration in the altered layer, i.e., substitution of an element of 2^+ oxidation state by an element of 4^+ oxidation state, which explains that in the final balance the O concentrations may stay constant. Second, it is very important to notice the preferential loss of Pb during 4 keV Ar^+ sputtering. Otherwise, incorrect conclusions could be drawn as, for instance, segregation of Pb to the film surface only attributed by other authors to the thermal treatment[35,36] and not to the effect of the Ar^+ bombardment during the XPS measurements.

Concluding Remarks

XPS combined with Ar^+ depth profiling is an useful tool for studying composition profiles, chemical changes, and interface reactions of sol−gel Pb−perovskite thin films on silicon-based substrates. For the correct interpretation of the XPS results, special care has to be taken with the preferential sputtering of Pb and reduction of oxides of the film during the Ar^+ bombardment. By taking into account these considerations, a quantitative control of the composition of the films by XPS can be deduced from the atomic ratios measured at the cleaned film surfaces. Further bombardment gives us the depth profile homogeneity of the films. Rapid heating crystallizations combined with appropriate Pb excesses led to Ca−$PbTiO_3$ films with a well-defined ferroelectric response that had the expected perovskite composition and a homogeneous depth profile.

Acknowledgment. This work has been partially supported by the Spanish Project MAT98-1068.

CM980770Y

(34) Moulder, J. F.; Stickle, W. F.; Sobol, P. E; Bomben, K. D. In *Handbook of X-ray Photoelectron Spectroscopy*; Chastian, J, Ed.; PHI: Eden Prairie, MN, 1992.

(35) Dana, S. S.; Etxold, K. F.; Clabes F. *J. Appl. Phys.* **1991**, *243*, 4398.

(36) Bozack, M. J.; Williams, J. R.; Ferraro, J. M.; Feng, Z. C.; Jones, R. E., Jr. *J. Electrochem. Soc.* **1995**, *142* (2), 485.